Coordination Chemistry of Microbial Iron Transport Compounds. 21. Kinetics and Mechanism of Iron Exchange in Hydroxamate Siderophore Complexes[1]

Thomas P. Tufano and Kenneth N. Raymond*

Contribution from the Department of Chemistry, University of California, Berkeley, California 94720. *Received February 27, 1981. Revised Manuscript Received July 6, 1981*

Abstract: The kinetics of iron exchange and iron removal from two siderophore complexes have been examined, using ^{55}Fe labeling techniques and UV–vis spectrophotometric methods, respectively. Iron exchange between the ferric complexes of ferrioxamine B ($FeHDFO^+$) and ferrichrome A ($FeDFC^{3-}$), two trihydroxamate siderophores from microbial cultures, is extremely slow; under conditions where there is a 5% excess of H_4DFO^+ per $FeHDFO^+$, the half-time for exchange for equimolar concentrations (4.0 mM) of the two complexes at 25 °C and pH 7.4 is approximately 220 h. The kinetics reveal an apparent first-order dependence of the rate on each of the competing metal complexes, with the exchange proceeding through a chain reaction involving free ligand. Furthermore, pH dependence studies demonstrate that the exchange rate is accelerated as a function of increasing hydrogen ion concentration. Kinetics of iron removal from ferrioxamine B with use of ethylenediaminetetraacetic acid (EDTA) show first-order dependence on the concentrations of the iron complex and hydrogen ion at 25 °C, with a pseudo-first-order rate constant of 4.8×10^{-5} s^{-1} at pH 5.4. Variation of the initial rate with EDTA concentration shows saturation kinetics at high ligand concentrations. The results are interpreted in terms of a two-step mechanism involving: (1) protonation of the ferrioxamine B complex and (2) subsequent bimolecular reaction with EDTA. Results of kinetic studies of the reverse process are consistent with the known equilibrium constants and microscopic reversibility. The reaction is first-order in the FeEDTA complex and desferrioxamine B. Although essentially no pH dependence is observed for this reverse process between pH 4 and 6, the reaction rate varies inversely with hydrogen ion concentration above pH 6. This is explained by consideration of the acid–base equilibria associated with the reactants, which give rise to multiple pathways for product formation. Specifically, the deprotonated form of the ferric–EDTA complex, $Fe(OH)EDTA^{2-}$, displays faster reaction kinetics with desferrioxamine B than does its conjugate acid form. A comparison of observed rate constants for the forward and reverse processes with known equilibrium constants shows good agreement. The postulated mechanisms for siderophore mediated microbial iron transport are evaluated in terms of the rates of iron exchange observed in these experiments.

Iron is an essential nutrient for microorganisms, as well as virtually all other organisms, because of its varied functions in biological redox processes: the transport of oxygen, the metabolism of inorganic nitrogen compounds, electron transport, and oxygen insertion reactions are a few examples. However, ferric ion, the major source of iron available in biological systems, is quantitatively insoluble as the hydroxide at physiological pH. Therefore, in response to an absolute requirement for iron, but at the same time limited by the insolubility of $Fe(OH)_3$ ($K_{sp} \sim 2 \times 10^{-39}$), microbes have evolved low-molecular-weight chelating agents, called siderophores, to solubilize and transport ferric ion in aqueous media. The general properties of this class of compounds[2-10] and the role of iron in microbial physiology[11] have been the subject of several reviews.

The ferrioxamines and ferrichromes constitute two important classes of siderophores. Ferrioxamine B (Figure 1A), produced by *Streptomyces pilosus*,[11] is a linear trihydroxamic acid whose basic structural feature is alternating units of 1-amino-5-(hydroxyamino)pentane and succinic acid. While ferrichrome A (Figure 1B), whose cyclic hexapeptide backbone provides a platform for the three hydroxamate moieties, is produced by the fungus *Ustilago sphaerogena*.[11] Both siderophores form extremely stable 1:1 coordination compounds with ferric ion, with formation constants on the order of 10^{30}. As a result of its high affinity for ferric ion, Desferal, the mesylate salt of desferrioxamine B, is currently the drug of choice (co-administered with ascorbic acid) for the clinical treatment of individuals suffering from acute iron toxicity (usually infant poisoning) or chronic iron overload[12,13] (as occurs in patients requiring massive, periodic blood transfusions for the treatment of blood disorders such as Cooley's anemia).

For some time we have been interested in the coordination chemistry of the siderophores and structurally related compounds. These studies have included X-ray structure determinations,[1,14,15] potentiometric titrimetry,[16] electrochemical studies,[17] and isomer assignment by spectrophotometric techniques.[18] However, one aspect of this chemistry which has received relatively little attention is the mechanism for iron exchange by siderophores.

It has been assumed that ferric ion is readily exchanged in siderophore complexes. For example, Lovenberg et al. observed a half-time of approximately 10 min for the exchange of $^{59}Fe^{3+}$ between ferric citrate and ferrichrome (Figure 1B).[19] This notion is consistent with the well-known substitutional lability of high-spin d^5 iron(III) in coordination complexes.[20] (More recently, Emery and Hoffer have reported the rapid exchange of gallium(III) citrate with ferrichrome A and Fe(III) nitrilotriacetate with gallium(III) deferriferrichrome A.[21]) However, observations in

(1) Previous paper in this series: Abu-Dari, K.; Raymond, K. N. *Inorg. Chem.* **1980**, *19*, 2034.
(2) Neilands, J. B. *Inorg. Biochem.* **1973**, 167.
(3) Lankford, C. E. *CRC Crit. Rev. Microbiol.* **1973**, *2*, 273.
(4) Hunter, S. H. *Annu. Rev. Microbiol.* **1972**, *26*, 313.
(5) Snow, G. A. *Bacteriol. Rev.* **1970**, *34*, 100.
(6) Pollack, J. R.; Neilands, J. B. *Biochem. Biophys. Res. Commun.* **1970**, 38, 989.
(7) O'Brien, I. G.; Gibson, F. *Biochim. Biophys. Acta* **1970**, *215*, 393.
(8) Emery, T. *Adv. Enzymol. Relat. Areas Mol. Biol.* **1971**, *33*, 135.
(9) Raymond, K. N. *Adv. Chem. Ser.* **1977**, *No. 162*.
(10) Raymond, K. N.; Carrano, C. J. *Acc. Chem. Res.* **1979**, *12*, 183.
(11) Neilands, J. B., Ed. "Microbial Iron Metabolism"; Academic Press: New York, 1974.
(12) Jacobs, A. *Brit. J. Haematol.* **1979**, *43*, 1.
(13) Hussain, M. A. M.; Flynn, D. M.; Green, N.; Hoffbrand, A. V. *Lancet* **1977**, *1*, 977.
(14) Raymond, K. N.; Abu-Dari, K.; Sofen, S. R. *Adv. Chem. Ser.* **1980**, *No. 119*, 133–167.
(15) Raymond, K. N.; Isied, S. S.; Brown, L. D.; Fronczek, F. R.; Nibert, J. H. *J. Am. Chem. Soc.* **1976**, *98*, 1767.
(16) Harris, W. R.; Carrano, C. J.; Raymond, K. N. *J. Am. Chem. Soc.* **1979**, *101*, 2722.
(17) Carrano, C. J.; Cooper, S. R.; Raymond, K. N. *J. Am. Chem. Soc.* **1979**, *101*, 599.
(18) Isied, S. S.; Kuo, G.; Raymond, K. N. *J. Am. Chem. Soc.* **1976**, *98*, 1763.
(19) Lovenberg, W.; Buchanan, B. B.; Rabinowitz, J. C. *J. Biol. Chem.* **1963**, *236*, 3899.
(20) Basolo, F.; Pearson, R. G. "Mechanisms of Inorganic Reactions", 2nd ed.; John Wiley and Sons, Inc.: New York, 1967; p 136 and 152.

0002-7863/81/1503-6617$01.25/0

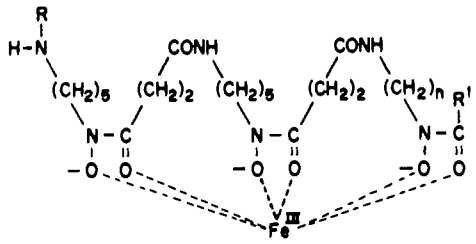

A

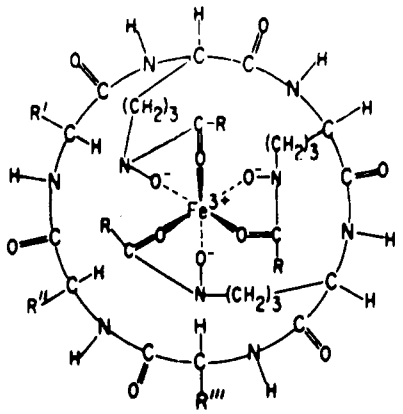

B

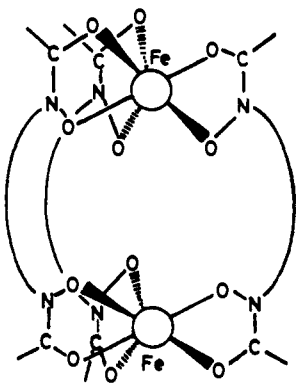

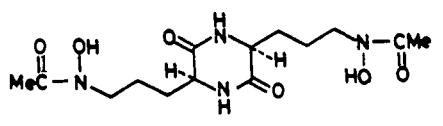

C

Figure 1. Structural formulas for three examples of hydroxamate siderophores of natural origin: (A) ferrioxamine B, R = H, R′ = $-CH_3$, n = 5; (B) ferrichrome A, R = $-CH{=}C(CH_3)-CH_2CO_2H$ (trans), R′ = R″ = $-CH_2OH$, R‴ = H; ferrichrome, R = $-CH_3$, R′ = R″ = R‴ = H; (C) ferric rhodotorulate.

our laboratory indicate that this assumption is *not* correct in general. For instance, the tris(hydroxamato) and tris(thiohydroxamato) complexes of high spin iron(III) have been resolved into their component optical isomers and have been found to be very stable in various nonaqueous solvents.[22,23] Specifically, more than 95% of the optical activity of the tris(benzhydroxamato)iron(III) complex is retained after *1 week* in acetone solution at room temperature! Certainly siderophores of natural origin, with the enhanced structural stability of three linked hydroxamate moieties, might be expected to exhibit unusually slow substitution kinetics for an iron(III) coordination complex, even though in an aqueous environment.

In this paper the rate of Fe^{3+} exchange between ferrioxamine B ($FeHDFO^+$) and ferrichrome A ($FeDFC^{3-}$) is examined under conditions of varying concentrations of both competing complexes and pH. That is, the kinetics for the equilibration:

$$*FeHDFO^+ + FeDFC^{3-} \rightleftharpoons FeHDFO^+ + *FeDFC^{3-} \quad (1)$$

are studied with use of ^{55}Fe labeling techniques. Such experiments provide mechanistic information about the exchange process, as well as a determination of the on–off rate for tightly bound siderophores at an iron center. In addition to these studies, much of this report will deal with the rate and mechanism of the uncatalyzed iron release from ferrioxamine B to EDTA. The overall reaction describing the iron removal process is:

$$FeHDFO^+ + H_2EDTA^{2-} + H^+ \rightleftharpoons FeEDTA^- + H_4DFO^+ \quad (2)$$

This represents the first in a series of experiments which will probe, in a systematic fashion, the kinetics and mechanism of iron extraction from a siderophore complex by a competing free ligand. This information provides a test for models of siderophore-mediated microbial iron transport,[24] which must be consistent with the mechanism proposed for the rapid removal of iron from siderophores in vivo.

Many mechanisms for siderophore-mediated microbial iron transport can be envisioned; Leong and Neilands[24] have summarized three limiting types. Mechanism 1 involves release of iron at the cell membrane without penetration of the iron complex or free ligand into the cell. Presumably the iron is released to a membrane-bound chelating agent which completes transport into the cell. The uptake of ferric rhodotorulate (Figure 1C) by *Rhodotorula pilimanae* appears to utilize this mechanism.[25] The salient feature of mechanism 2 is the uptake of the iron siderophore complex followed by intracellular iron release and re-excretion of the free ligand. Emery[26] has demonstrated that ferrichrome acts as a true cell permease in this manner for *Ustilago sphaerogena*. Mechanism 3 involves transport of the intact iron complex, but once inside the cell, iron is released through chemical degradation of the ligand. For example, the transport of ferric ion by enterobactin (a tricatecholate siderophore) apparently follows this mechanism. It is believed that cleavage of the ester backbone of the ligand by a specific esterase is necessary for iron removal from the complex.[27,28]

Iron transport studies involving isomers of chromic/desferrioxamine B have been performed.[24] In this work, the uptake of ^{55}Fe and ^{3}H labeled ferrioxamine B and the cis and trans isomers of substitutionally inert chromic [^{3}H]desferrioxamine B in *Salmonella typhimurium* LT-2 emb7 were monitored. *Salmonella typhimurium*, which does not produce deferrioxamine B, is nonetheless capable of using this siderophore as an iron transport agent. These results, along with those of the ferrioxamine B iron removal kinetics reported here, will be interpreted in terms of a probable scheme for the rapid removal of iron from this siderophore complex.

Experimental Section

Preparation of Solutions. Desferal was used as received from CIBA Pharmaceuticals. The disodium salt of EDTA, obtained from Pfaltz and Bauer, Inc., was employed without further purification. Ferrichrome A was a generous gift from Professor J. B. Neilands of this University. Stock solutions of the metal complexes and the free ligands were prepared with use of 0.10 M tris(hydroxymethyl)aminomethane (Tris) buffer, ionic

(21) Emery, T.; Hoffer, P. B. *J. Nucl. Med.* **1980**, *21*, 935.
(22) Abu-Dari, K.; Raymond, K. N. *Inorg. Chem.* **1977**, *16*, 807.
(23) Abu-Dari, K.; Raymond, K. N. *J. Am. Chem. Soc.* **1977**, *99*, 2003.
(24) Leong, J.; Raymond, K. N. *J. Am. Chem. Soc.* **1975**, *97*, 293. Leong, J.; Neilands, J. B. *J. Bacteriol.* **1976**, *126*, 823.
(25) Carrano, C. J.; Raymond, K. N. *J. Bacteriol.* **1978**, *136*, 69.
(26) Emery, T. *Biochemistry* **1971**, *10*, 1483.
(27) O'Brien, I. G.; Cox, C. B.; Gibson, F. *Biochim. Biophys. Acta* **1971**, *237*, 537.
(28) Langman, L.; Young, I. G.; Frost, G. E.; Rosenberg, H.; Gibson, F. *J. Bacteriol.* **1972**, *112*, 1142.

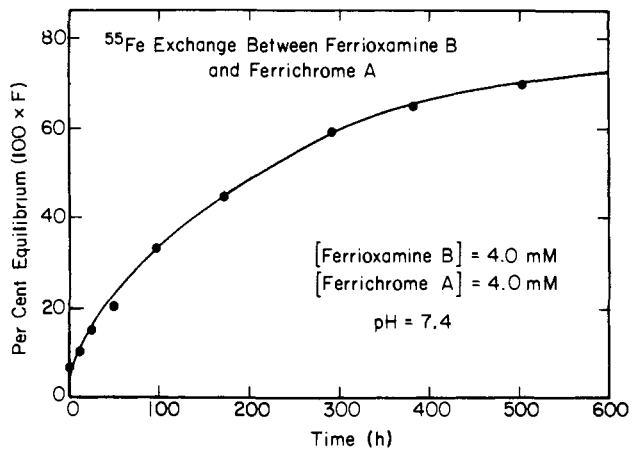

Figure 2. Reaction profile for exchange of iron between ^{55}Fe-labeled ferrioxamine B and ferrichrome A. The quantity F is the fractional degree to which equilibrium has been reached.

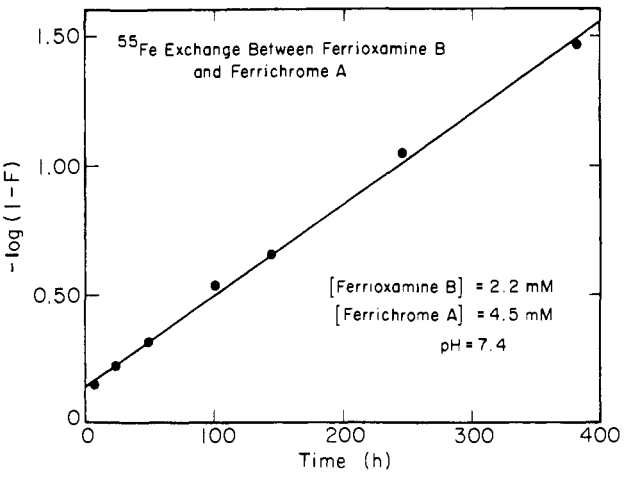

Figure 3. Characteristic linear plot of the quantity $-\log(1 - F)$ vs. time for the exchange of the ^{55}Fe label.

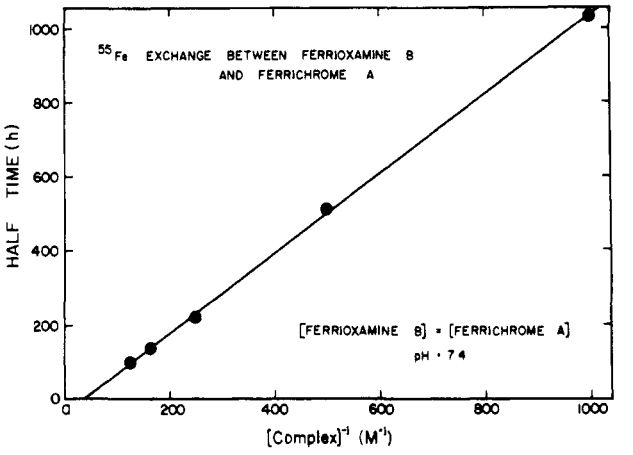

Figure 4. The linear relationship between the half-time for iron exchange between ferrioxamine B (and the free desferrioxamine B, which is in 5% excess) and ferrichrome A and the reciprocal of their concentration.

strength = 0.2 M (KNO_3). Iron was introduced into stock solutions by using a standardized (0.08946 M) ferric nitrate solution prepared according to literature procedures.[29] Typically, 5% excess ligand was used to ensure complete complexation of the ferric ion. When necessary, final pH adjustments were made with use of freshly prepared, concentrated KOH and HNO_3 solutions. All pH measurements were made with use of a Beckman Instruments Model pH-102 digital meter equipped with a glass calomel combination electrode (Sigma). Solutions were refrigerated at 4 °C prior to use.

$^{55}Fe^{3+}$ Exchange Experiments. Reaction mixtures (buffered solutions of ferrioxamine B and ferrichrome A, 2.2 mL in total volume) in screw capped vials wrapped with parafilm were maintained in a constant temperature water bath (25.0 ± 0.05 °C) throughout the experiment. A small fraction of the iron in the ferrioxamine B stock solution was labeled with use of $^{55}FeCl_3$. The time of mixing was taken as time zero. Ten 0.20-mL aliquots of the reaction mixture were removed from each reaction vial as a function of time. Each aliquot was passed over a cation exchange column packed with Biorad AG 50W-X8, 100–200 mesh resin in the hydrogen form. Columns were typically 0.5 cm in diameter and 2–3 cm in length. Ferrioxamine B, with its unipositive charge, adhered quantitatively to the resin while ferrichrome A (trinegative charge on complex) passed cleanly through the column. Separation of the components was complete within 15–30 s. The eluant was subsequently diluted with distilled water to 10 mL total volume. A 0.4-mL aliquot of each solution was then diluted with approximately 10 mL of nonaqueous scintillation fluid and counted on a tritium channel, using a Searle Isocap/300 liquid scintillation counter. For each exchange experiment controls were employed to ensure: (1) the quantitative retention of the labeled ferrioxamine B on the cation exchange resin, (2) the background counts associated with an unlabeled ferrichrome A solution, and (3) the maximum number of counts that could be anticipated when the reaction reached equilibrium. Plots of percent equilibrium vs. time served to indicate the progress of reaction.

Iron Release from Ferrioxamine B. Visible spectrophotometric studies were carried out with use of a Cary 118 UV–vis spectrophotometer at λ 428 nm. Quartz cells with 1 cm optical pathlength were thermostated at 25.0 ± 0.05 °C for all experiments. Reaction mixtures were typically 2.4 mL in total volume and millimolar concentrations of metal complex and free ligand were employed in all cases. The method of initial rates, coupled with linear least-squares refinement, was applied to absorbance vs. time data sampled for the first 1% of the reaction time.[30] Absorbance measurements were made after 3–5 days to determine the point of equilibrium. The buffers used for pH dependence studies included 0.10 M Tris-acetate, 2-(*N*-morpholino)ethanesulfonic acid (MES), and Tris-HCl.

Results

$^{55}Fe^{3+}$ Exchange between Ferrioxamine B and Ferrichrome A. The exchange of labeled iron between these two complexes of hexadentate siderophores is an extremely slow process. As Figure 2 illustrates, the reaction is only 50% complete after 220 h of incubation at 25 °C and pH 7.4 for equimolar concentrations of the competing complexes with 5% excess H_4DFO^+. These data have been analyzed in terms of the general first-order relationship[31] characteristic of isotope exchange processes:

$$-\ln(1 - F) = (R/ab)(a + b)t \qquad (3)$$

where a and b represent the total concentrations of the two iron siderophore complexes: R is the gross rate of exchange of all iron atoms (without regard to isotope mass), a function of a and b, and a constant for a given run; and F is the fraction of exchange that has occurred in the time t, i.e., $F = 1$ at $t = \infty$. A typical plot of $-\ln(1 - F)$ vs. time for the ferrioxamine B–ferrichrome A exchange reaction is shown in Figure 3. The linear relationship holds for a substantial portion of the reaction time and provides a convenient check for the experimental data. In order to determine the dependence of the rate, R, on the concentrations of ferrichrome A and ferrioxamine B, several runs were carried out at varied concentrations of the two siderophore complexes. The results reveal that the rate of iron exchange is apparently first order with respect to each iron complex, that is, $R = k_{2(exch)}$[ferrioxamine B][ferrichrome A] at pH 7.4. Note that since the free ferrioxamine B ligand concentration is always proportional (5%) to [$FeHDFO^+$] an equivalent form for this equation is $R = k_2$[Fe complex][free H_4DFO^+]. As will be described, the latter conforms to the proposed mechanism. The overall second-order dependence at constant pH is precisely reflected by the linear relationship between the half-time for iron exchange and the

(29) Welcher, F. J. "Analytical Uses of Ethylenediaminetetraacetic Acid"; D. Van Nostrand Company, Inc.: New York, 1958.
(30) Wilkins, R. G. "The Study of Kinetics and Mechanism of Reactions of Transition Metal Complexes"; Allyn and Bacon, Inc.: Boston, 1974; p 5.
(31) Frost, A. A.; Pearson, R. G. "Kinetics and Mechanism", 2nd ed.; John Wiley and Sons, Inc.: New York, 1961; p 192.

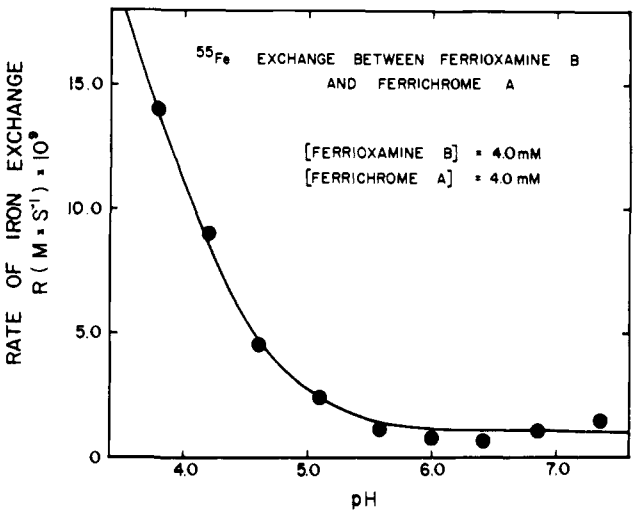

Figure 5. The dependence of the ^{55}Fe exchange rate, R, on pH.

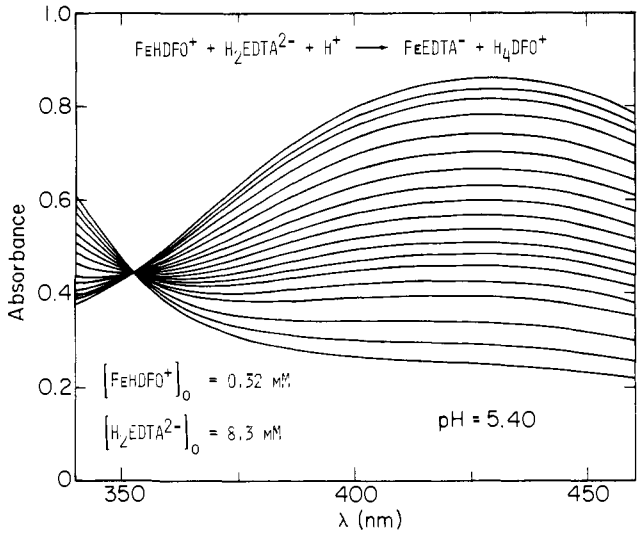

Figure 6. Spectral changes accompanying iron removal from ferrioxamine B by ethylenediaminetetraacetic acid (EDTA).

reciprocal of the complex concentration as shown in Figure 4. Figure 5 shows the dependence of R on pH. The rate of iron exchange is relatively constant between pH 5.5 and 7.4. However, as the hydrogen ion concentration is increased below pH 5, a sharp increase in the exchange rate is observed. Specifically, the data reveal that at pH 3.8, the half-time is reduced to 24 h.

Kinetics and Mechanism of Iron Release from Ferrioxamine B. The spectral changes observed when ferrioxamine B is added to a buffered solution of EDTA are shown in Figure 6. The top trace (t = 1.0 min) corresponds essentially to the spectrum of unreacted ferrioxamine B. Subsequent spectra illustrate the decrease in absorbance at 428 nm due to ferrioxamine B ($FeHDFO^+$), with a concomitant increase in the UV absorption (not shown) of the product, ethylenediaminetetraacetatoferrate-(III) anion ($FeEDTA^-$). The isosbestic point at 352 nm indicates the presence of two absorbing species in solution as equilibrium is approached. These are the initial reactant, $FeHDFO^+$, and the final product, $FeEDTA^-$. The time elapsed between the first and last spectral traces is approximately 8 h, at which time approximately 70% of the iron has been removed.

Figures 7 and 8 illustrate the first-order dependence of the initial rate on the concentration of $FeHDFO^+$ and H^+, respectively. From the slope of the line in Figure 7, a pseudo-first-order rate constant (k_{obsd}) of 4.8 (2) $\times 10^{-5}$ s^{-1} is obtained.[32] Although in

(32) Estimated standard deviations in the least significant digits of numerical results are presented in parentheses.

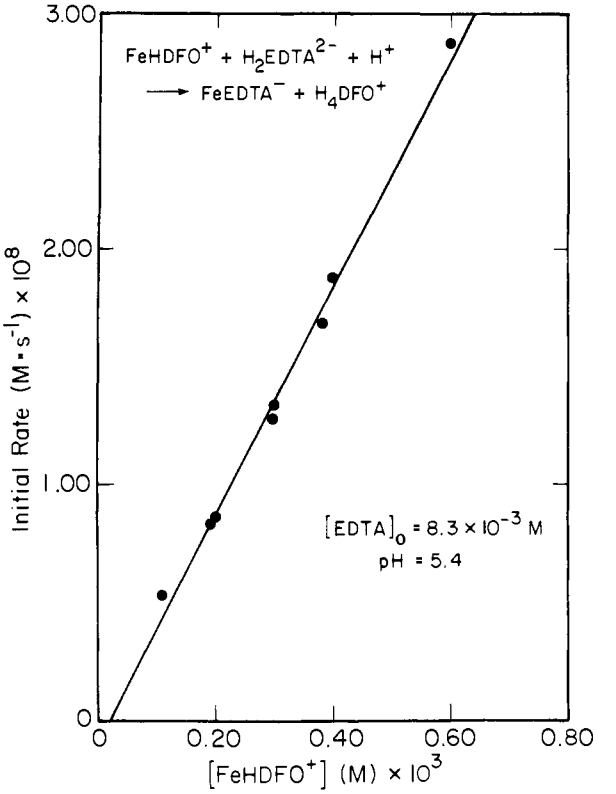

Figure 7. Plot of the initial rate for iron removal from ferrioxamine B vs. the concentration of ferrioxamine B.

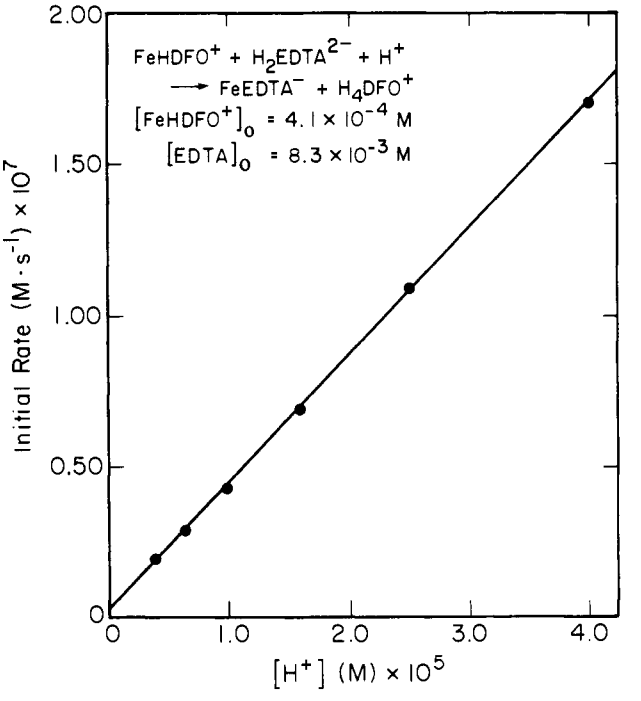

Figure 8. The dependence of the initial rate for iron removal from ferrioxamine B on hydrogen ion concentration.

Figure 8 data are shown only for a pH range of 4.4–5.4, the linear relationship holds up to physiological pH (where the rate of iron removal is drastically reduced). From a plot of ln [$FeHDFO^+$] vs. time, an independent determination of k_{obsd} can be made. The value obtained, 4.6 (1) $\times 10^{-5}$ s^{-1}, is in good agreement with that derived from the initial rates study.

Figure 9 shows the dependence of the initial rate on the initial concentration of EDTA. Saturation kinetics are observed for high concentrations of the entering ligand. The small degree of curvature in this plot indicates that the EDTA concentration range

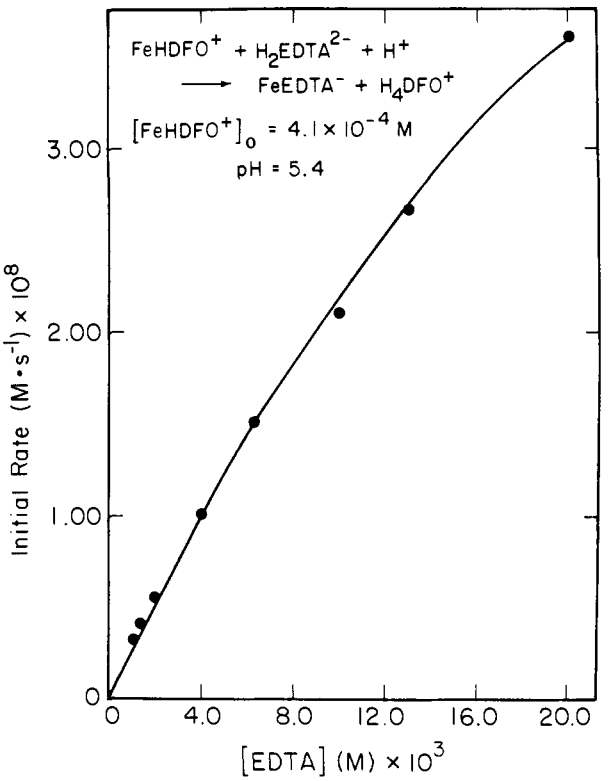

Figure 9. EDTA dependence of the initial rate for iron removal from ferrioxamine B.

chosen in somewhat less than optimal. That is, the highest EDTA concentration employed does not give rise to complete saturation and a constant maximal rate. The curve represents a nonlinear least-squares fit of the data based upon the proposed mechanism for iron release (vide infra).

A mechanism which is consistent with the kinetic observations presented thus far is given by eq 4 and 5. The competing EDTA

$$FeHDFO^+ + H^+ + 2H_2O \underset{k_{-1}}{\overset{k_1}{\rightleftharpoons}} Fe(H_2DFO)(H_2O)_2^{2+} \quad (4)$$

$$Fe(H_2DFO)(H_2O)_2^{2+} + H_2EDTA^{2-} \xrightarrow{k_2} FeEDTA^- + H_4DFO^+ + 2H_2O \quad (5)$$

$$FeHDFO^+ + H_2EDTA^{2-} + H^+ \overset{K_{eq}}{\rightleftharpoons} FeEDTA^- + H_4DFO^+ \quad \text{(overall)}$$

species is explicitly written in the diprotonated form, since this is the predominant species in solution at pH 5.4. However, it is recognized that the free ligand species, $HEDTA^{3-}$ and H_3EDTA^-, can also lead to product formation in the second step of the mechanism. Thus a set of three parallel reaction pathways in place of eq 5 would represent a more complete formulation of the kinetics over the pH range 4.4–7.4. Since the hydrogen ion dependence is essentially first order over the entire pH range studied, consideration of the detailed acid dependence in eq 5 is omitted, and k_2 is therefore an observed rate constant for the reaction of a H_xEDTA^{x-4} species with $Fe(H_2DFO)(H_2O)_2^{2+}$. A calculation of the concentration of the proposed intermediate, $Fe(H_2DFO)(H_2O)_2^{2+}$, at pH 5.4, using known equilibrium data at 25 °C,[33] yields a value of $\sim 10^{-8}$ M. Even if this did not give an upper limit (as it does) to the concentration of the bis(aquo)bis(hydroxamato)iron(III) species, it must be present in low, steady-state concentration throughout the course of the reaction, since as a third absorbing species it would destroy the observed isosbestic point if present in significant concentration. Therefore

(33) Pecoraro, V. L.; Raymond, K. N., unpublished results.

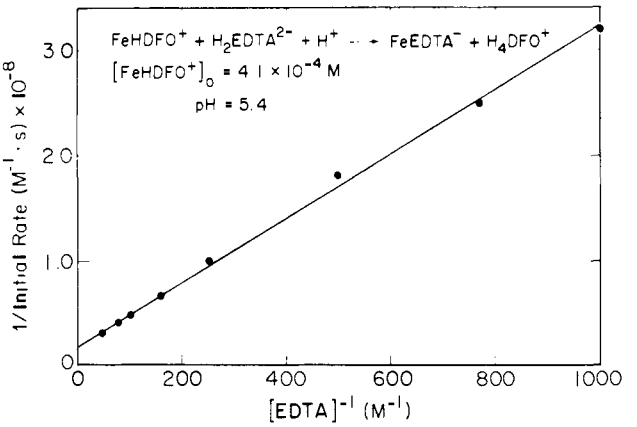

Figure 10. The linear, double-reciprocal relationship between the initial rate for iron removal from ferrioxamine B and the concentration of EDTA.

a steady-state approximation is justified and leads to the following rate expression.

$$V_{initial} = -\frac{d[FeHDFO^+]}{dt} = \frac{k_1k_2[FeHDFO^+][H^+][H_2EDTA^{2-}]}{k_{-1} + k_2[H_2EDTA^{2-}]} \quad (6)$$

$$\frac{1}{V_{initial}} = \frac{k_{-1}}{k_1k_2[FeHDFO^+][H^+]}\left(\frac{1}{[H_2EDTA^{2-}]}\right) + \frac{1}{k_1[FeHDFO^+][H^+]} \quad (7)$$

Equation 7 suggests that a plot of $1/V_{initial}$ vs. $1/[H_2EDTA^{2-}]$ should be linear (Figure 10). From the slope and intercept, and a knowledge of the equilibrium constant at 25 °C for eq 4 above ($K = k_1/k_{-1} = 10$),[33] the following values for k_1, k_{-1}, and k_2 are obtained: $k_1 = 34$ (5) M^{-1} s^{-1}, $k_{-1} = 3.4$ (9) s^{-1}, and $k_2 = 200$ (10) M^{-1} s^{-1}.

Kinetics and Mechanism of Iron Release to Ferrioxamine B. To lend support of the analysis presented above, the kinetics and mechanism of the reverse reaction were also studied. The observed kinetics for the extraction of iron from $FeEDTA^-$ by desferrioxamine B (H_4DFO^+) are compared to predictions made on the basis of the principle of microscopic reversibility and the known equilibrium. This predicts that the bimolecular reaction between $FeEDTA^-$ and H_4DFO^+ should be rate determining, and no hydrogen ion dependence is anticipated. The linear dependence of the initial rate on the concentrations of $FeEDTA^-$ and H_4DFO^+ is shown in Figures 11 and 12, respectively. The results of the pH dependence study are shown in Figure 13. There is essentially no dependence on hydrogen ion concentration over the pH range 4.0–6.0. Above pH 6, however, a profound inverse dependence between initial rate and H^+ concentration is observed. These results can be explained when one considers the acid–base equilibria of the reactants:

$$Fe(OH)(EDTA)^{2-} + H^+ \overset{K_H}{\rightleftharpoons} Fe(H_2O)(EDTA)^- \quad (8)$$

$$H_3DFO + H^+ \overset{K_H'}{\rightleftharpoons} H_4DFO^+ \quad (9)$$

The ferric–EDTA complex is now explicitly written as $Fe(H_2O)(EDTA)^-$ to emphasize the acid–base behavior. The stereochemistry of the seven-coordinate $Fe(H_2O)(EDTA)^-$ anion has been established by single-crystal X-ray structure analysis.[34]

(34) Hoard, J. L.; Lind, M.; Silverton, J. V. *J. Am. Chem. Soc.* **1961**, *83*, 2770.

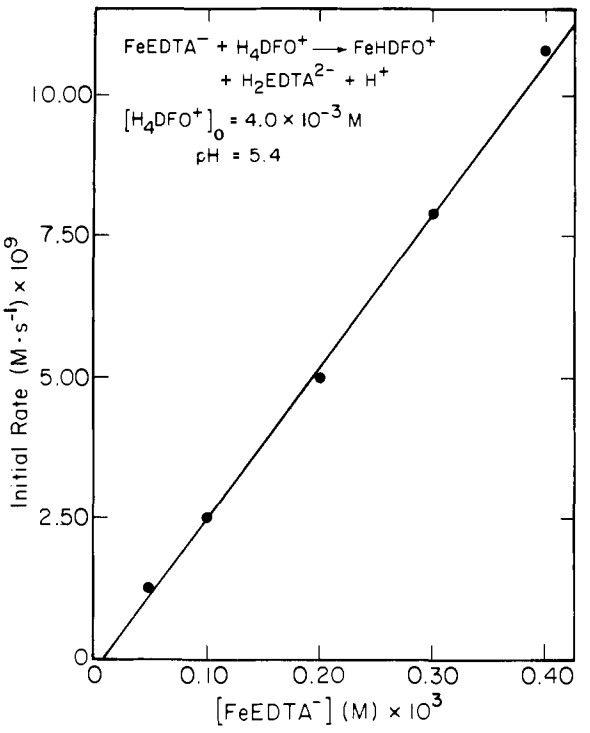

Figure 11. Plot of initial rate for iron removal from ferric-EDTA vs. the concentration of the ferric-EDTA complex.

Over the pH range 4.0–8.0 four possible pathways leading to product formation are operative:

$$Fe(H_2O)(EDTA)^- + H_4DFO^+ \xrightarrow{k_{AH_2}} \text{products} \quad (10)$$

$$Fe(OH)(EDTA)^{2-} + H_4DFO^+ \xrightarrow{k_{AH}} \text{products} \quad (11)$$

$$Fe(H_2O)(EDTA)^- + H_3DFO \xrightarrow{k_{AH'}} \text{products} \quad (12)$$

$$Fe(OH)(EDTA)^{2-} + H_3DFO \xrightarrow{k_A} \text{products} \quad (13)$$

The rate of product formation can then be expressed by the following rate expression,

$$\text{rate} = \frac{d[FeHDFO^+]}{dt} = k_{obsd}'[Fe(H_2O)(EDTA)^-][H_4DFO^+] \quad (14)$$

where k_{obsd}' is a function of the hydrogen ion concentration and specific rate constants. An analysis of eq 8–13 reveals that k_{obsd}' is of the form

$$k_{obsd}' = a + b/[H^+] + c/[H^+]^2 \quad (15)$$

with

$$a = k_{AH_2} = 5.9\ (9) \times 10^{-3}\ M^{-1}\ s^{-1}$$

$$b = k_{AH}/K_H + k_{AH}'/K_H' = 1.8\ (2) \times 10^{-9}\ s^{-1}$$

$$c = k_A/(K_H K_H') = 2.2\ (2) \times 10^{-17} M\ s^{-1}$$

By using least-squares refinement of the coefficients in eq 15, the initial rates vs. pH data can be fit with use of eq 14. The smooth curve in Figure 13 represents the results of this fit. Based upon the refined values for the coefficients, a and c, and the equilibrium formation constants (K_H and K_H') for eq 8 and 9,[33,35] the magnitude of the rate constants, k_{AH_2} and k_A, can be determined unambiguously. The values are $k_{AH_2} = 5.9\ (9) \times 10^{-3}\ M^{-1}\ s^{-1}$ and $k_A = 1.1\ (1) \times 10^{-1}\ M^{-1}\ s^{-1}$. Independent values for k_{AH} and k_{AH}' cannot be determined because they represent reaction paths that differ only in transfer of a proton from the metal complex to the siderophore ligand. From the results summarized by Figures 11, 12, and 13, the value for the observed bimolecular rate constant (k_{obsd}') at pH 5.4 is 6.6 (8) $\times 10^{-3}\ M^{-1}\ s^{-1}$.

The ratio k_2/k_{obsd}' should be in agreement with the calculated equilibrium constant[33,35] for eq 5 above. The observed and calculated values are 3.0 (4) $\times 10^{+4}$ and 2.5 $\times 10^{+4}$, respectively.

(35) Martell, A. E.; Smith, R. M. "Critical Stability Constants"; Plenum Press: New York, 1977; Vol. 3, p 303.

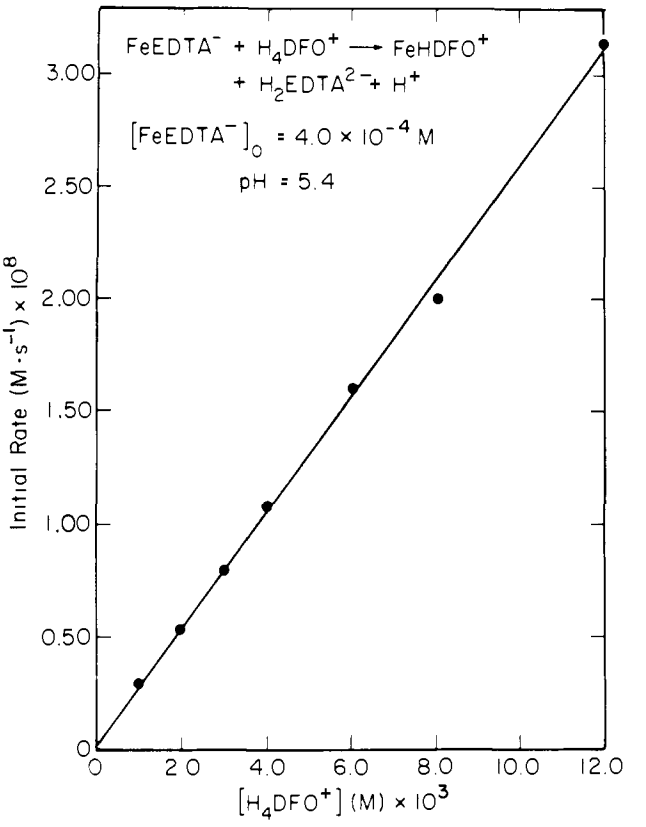

Figure 12. Desferrioxamine B dependence of the initial rate for iron removal from ferric-EDTA.

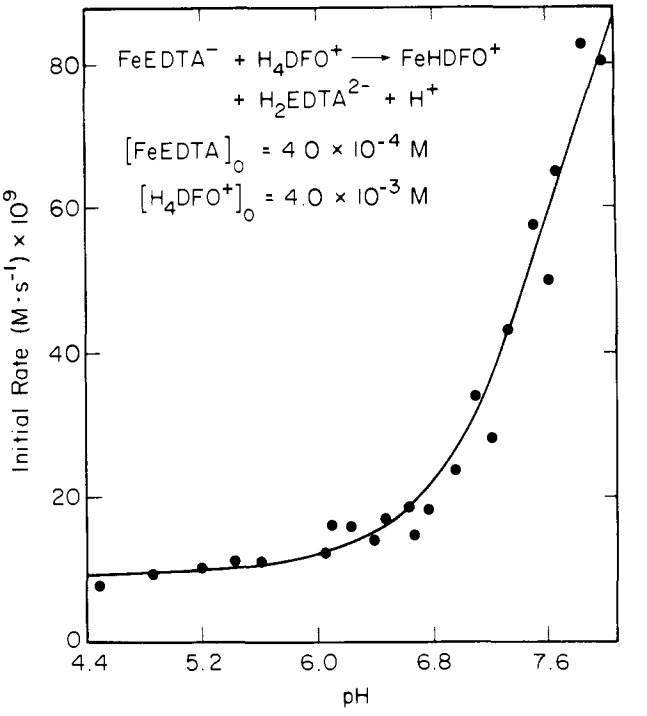

Figure 13. The dependence of the initial rate for iron removal from ferric-EDTA on pH. The points represent observed data and the curve is a nonlinear, least-squares fit.

Discussion

The mechanism for iron removal from ferrioxamine B by EDTA points out the importance of opening the coordination sphere about the iron center for subsequent attack by the competing ligand. Protonation of one hydroxamate functionality (eq 4) leads to the momentary formation of a bis(aquo)bis(hydroxamato)iron(III) species—a species known to exist in equilibrium at low pH.[36] The primary coordination sphere is thereby relatively exposed, through the partial unwrapping of the hexadentate ligand and the presence of the labile unidentate aquo ligands. Thus EDTA can gain a "coordination foothold"[37] on the iron center in forming a ternary complex of metal ion and entering and leaving ligands. Subsequent formation of the product (eq 5), ferric–EDTA, is driven to the right in the presence of excess EDTA, as the equilibrium constant of $2.5 \times 10^{+4}$ (given above) illustrates. It should be noted that eq 5 is simplified (in addition to the assumptions discussed above) in that k_2 is probably an observed constant composed of several pH-dependent rate constants associated with the formation and dissociation of a ternary, mixed ligand iron(III) complex similar to those for the reverse reactions (eq 10–13). Therefore in place of eq 5, one could more explicitly write:

$$Fe(H_2DFO)(H_2O)_2^{2+} + H_2EDTA^{2-} \underset{k_{-3}}{\overset{k_3}{\rightleftharpoons}} (H_2EDTA)Fe(H_2DFO) + 2H_2O \quad (16)$$

$$(H_2EDTA)Fe(H_2DFO) \xrightarrow{k_4} FeEDTA^- + H_4DFO^+ \quad (17)$$

In this respect, the detailed mechanism for iron extraction from a siderophore complex complements the results obtained in the ^{55}Fe exchange studies (discussed below). Although the kinetic data are consistent with the formation of a ternary complex, and these are known for other chelate substitution reactions of EDTA,[38-40] no direct evidence for the existence of a ternary complex is presented here.

While the data for the reverse reaction provide an internal check on the ferrioxamine B/EDTA kinetics, the results are also of interest when considered alone. The postulation of enhanced reactivity of the hydroxo species, $Fe(OH)EDTA^{2-}$, over that of $Fe(H_2O)EDTA^-$, is in accord with earlier studies. For example, Connick and Stover[41] and Connick and Genser[42] have determined that the second-order rate constant for water exchange on $Fe(H_2O)_6^{3+}$ is approximately $2.8 \times 10^{+2}$ M^{-1} s^{-1} at 25 °C. The same authors estimated that the exchange of water on $Fe(OH)(H_2O)_5^{2+}$ is roughly 100 times faster than that for $Fe(H_2O)_6^{3+}$. This has recently been confirmed by Grant and Jordan,[43] who used pulsed NMR techniques to obtain second-order rate constants of 1.6×10^2 M^{-1} s^{-1} and 1.4×10^5 M^{-1} s^{-1} for $Fe(H_2O)_6^{3+}$ and $Fe(OH)(H_2O)_5^{2+}$, respectively. Furthermore, it is generally found for unidentate ligand substitution that $Fe(OH)(H_2O)_5^{2+}$ reacts 10 to 1000 times faster than does $Fe(H_2O)_6^{3+}$.[42,43]

We find the difference in reactivity between $Fe(OH)EDTA^{2-}$ and $Fe(H_2O)EDTA^-$ is much less than that for the aquo species. For instance, the ratio k_A/k_{AH_2} is ~20, and the ratio k_{AH}/k_{AH_2} is predicted to be even smaller (assuming $k_A > k_{AH} \sim k_{AH'} > k_{AH_2}$). However, these relative rates *are* typical for ligand substitution involving multidentate ligands. For example, for the biomolecular reactions,

$$FeEDTA^- + {}^*Fe(H_2O)_6^{3+} \rightleftharpoons {}^*FeEDTA^- + Fe(H_2O)_6^{3+} \quad (18)$$

and

$$FeEDTA^- + {}^*Fe(OH)(H_2O)_5^{2+} \rightleftharpoons {}^*FeEDTA^- + Fe(OH)(H_2O)_5^{2+} \quad (19)$$

the rate constant for eq 19 is about 10 times larger (2.3×10^{-3} M^{-1} s^{-1} vs. 2.5×10^{-4} M^{-1} s^{-1}) than that observed for the reaction of the hexaaquoferric ion in eq 18.[44]

While the studies of the ^{55}Fe exchange rates between ferrioxamine B and ferrichrome A do not provide the same detail available from the EDTA/DFO kinetics, the ^{55}Fe exchange studies are consistent with the mechanism proposed for the EDTA/DFO system. We propose the same general mechanism is operative in both cases: a rate-determining formation of a ternary complex between metal ion and entering and leaving ligands. For the exchange between siderophore metal complexes in which the hexadentate properties of the ligands match the coordination number of the metal this means both free coordination sites on one complex and free ligand sites on a second must be generated in a step prior to ternary complex formation. Under the conditions of these experiments (that is, 5% excess H_4DFO^+ to ensure complete complexation of ferric ion with its $^{55}Fe^{3+}$ label), the second requirement of generation of free ligand sites is removed (or at best a minor contribution to the overall rate). Iron exchange is undoubtedly effected through a two-step chain reaction mechanism utilizing excess ligand:

$$FeDFC^{3-} + H_4DFO^+ \underset{k_{-1}}{\overset{k_1}{\rightleftharpoons}} FeHDFO^+ + H_3DFC^{3-} \quad (20)$$

$$^{55}FeHDFO^+ + H_3DFC^{3-} \underset{k_1}{\overset{k_{-1}}{\rightleftharpoons}} {}^{55}FeDFC^{3-} + H_4DFO^+ \quad (21)$$

Implicit in the formulation represented by eq 20 and 21 is the fact that a mixed ligand ternary complex is formed during the exchange of a single iron atom from desferrichrome A to desferrioxamine B. Certainly, given the large formation constants of these ligands for ferric ion, an exchange process that involves the complete dissociation of either siderophore complex [forming $Fe(H_2O)_6^{3+}$], followed by rapid complexation by the competing ligand, can be eliminated. Such a process is also inconsistent with prior work on multidentate ligand exchange. Rather, the rate-determining unraveling of one ligand from the inner coordination sphere, concomitant with complexation by the incoming ligand, is the predominant characteristic feature of the exchange process. In addition, predissociation is not required for initiation of the chain reaction mechanism in the presence of excess ligand.

The mechanism described in eq 20 and 21 is consistent with the early work of Olson and Margerum[45] on coordination chain reactions. For example, for the exchange of metal atoms between tris(ethylenetetramine)nickel(II) and (ethylenediaminetetraacetato)cuprate(II), small amounts of excess trien or EDTA have a pronounced catalytic effect on the rate of exchange.

In view of the protonation behavior of ferrioxamine B and ferrichrome A,

$$FeHDFO^+ + H^+ + 2H_2O \underset{}{\overset{K_H''}{\rightleftharpoons}} Fe(H_2DFO)(H_2O)_2^{2+} \quad (4)$$

$$FeDFC^{3-} + H^+ + 2H_2O \underset{}{\overset{K_H'''}{\rightleftharpoons}} Fe(HDFC)(H_2O)_2^{2-} \quad (22)$$

(assuming $K_H''' \approx K_H'' = 10.0$ M^{-1}) one would predict that exposing the inner iron coordination sphere to small, labile unidentate ligands (H_2O) through protonation would enhance the rate of subsequent multidentate ligand exchange. Lowering the pH of reaction mixtures increases the equilibrium concentration of bis(aquo)bis(hydroxamato)iron(III) species, and, as a consequence, several proton-dependent reaction pathways are operative. This is exactly what is observed experimentally in the iron exchange kinetics between the two siderophores (Figure 5). This illustrates that relatively rapid reaction kinetics (typically associated with high-spin ferric ion) can be observed in iron(III) exchange between tightly bound hexadentate siderophores by labilization (reducing the denticity of the ligand) of the metal center through protonation of the ligand. The experimental data in Figure 5 have not been fit to an explicit function of hydrogen ion concentration, since a number of parallel reaction pathways, analogous to those postu-

(36) Schwarzenbach, G.; Schwarzenbach, K. *Helv. Chim. Acta* **1963**, *46*, 1390.
(37) Rorabacher, D. B.; Margerum, D. W. *Inorg. Chem.* **1964**, *3*, 382.
(38) Margerum, D. W.; Rosen, H. M. *Inorg. Chem.* **1968**, *7*, 299.
(39) Carr, J. D.; Reiley, C. N. *Anal. Chem.* **1970**, *42*, 51.
(40) Bryson, A.; Fletcher, I. S. *Aust. J. Chem.* **1970**, *23*, 1095.
(41) Connick, R. E.; Stover, E. D. *J. Phys. Chem.* **1961**, *65*, 2075.
(42) Seewald, D.; Sutin, N. *Inorg. Chem.* **1963**, *2*, 643.
(43) Grant, M.; Jordan, R. B. *Inorg. Chem.* **1981**, *20*, 55.
(44) Jones, S. S.; Long, F. A. *J. Phys. Chem.* **1952**, *56*, 25.
(45) Olson, D. C.; Margerum, D. W. *J. Am. Chem. Soc.* **1963**, *85*, 297.

lated for the EDTA/DFO kinetics, are operative in this region.

In a previous study, Lovenberg et al.[19] found that metal ion transfer from ferric citrate to ferrichrome is relatively rapid ($t_{1/2} \sim 10$ min). This has been interpreted as indicating a generally rapid rate of iron exchange and transfer to and between siderophores. However, citrate is a bidentate ligand which, when present in the concentrations used in the Lovenberg experiment, forms a bis (two to one) complex with Fe(III). The reduced denticity of the citrate ligand and the ease with which its complex partially dissociates to give free coordination sites on the metal are consistent with the relatively rapid exchange observed for this system, but is in marked contrast to the dramatically slower rates observed in this study.

As described in the introduction of this paper, there are three limiting mechanisms of siderophore transport that have been proposed. In transport studies of labeled ferric and chromic complexes of ferrioxamine B by *Salmonella typhimurium*,[24] it was found that neither of the obtained chromic complex isomers was transported into the microbe, and the ^{55}Fe label was taken up more rapidly than the ^{3}H ligand label. Mechanism 3 (transport of intact complex and metal release by ligand destruction) does not pertain in this system, since the ferrioxamine B remains intact. Mechanism 2 (the active transport of the intact metal complex) seems unlikely, since neither chromic complex was transported. Only if it is hypothesized that another, not isolated, isomer is *specifically* absorbed can mechanism 2 be operative. This leaves mechanism 1 (involving ligand exchange at the cell surface) as the most likely process in this system, and requires a rapid rate of iron removal from ferrioxamine B in order to be consistent with the rapid uptake of ^{55}Fe (complete in 30 min) by *S. typhimurium*. Even if mechanism 2 were operative, a rapid mechanism for iron release by ferrioxamine B *inside* the cell is necessary. The results presented here show that the uncatalyzed extraction of iron from ferrioxamine B by EDTA is a relatively slow process (initial rate of 1.4×10^{-10} M s^{-1} at pH 7.4 and ~20:1 ratio of EDTA to $FeHDFO^{+}$)—a rate which is not consonant with the rate of iron uptake in ligand transport experiments. One probable mechanism for the release of iron from trihydroxamates (in addition to the effect of rate enhancement due to high hydrogen ion concentration) is reduction to the ferrous state, which converts the tightly bound ferric complex to the loosely bound ferrous complex, from which the iron can be easily extracted and the intact ligand can be recycled.[26] The feasibility of this mechanism has been established by electrochemical studies of the redox process.[46] An example of this type of metabolic pathway for iron is in the ferrichrome mediated iron transport in *U. sphaerogena*,[47] in which an NADH-dependent ferrichrome reductase (NADH:ferrichrome oxidoreductase) is thought to be active in iron release from this siderophore. Further examples of reductase activity in the catalytic removal of iron from siderophores[48,49] and iron storage proteins[50] can be found in the literature.

In summary, iron release from the trihydroxamate siderophores ferrichrome A and ferrioxamine B is very slow at physiological pH. It is very likely this is generally true for all of the hexadentate siderophores. Since siderophore-mediated iron transport and release is a much more rapid process than the simple exchange kinetics of these Fe(III) complexes, the role of redox reactions in the catalysis of this exchange comes into question. Experiments to elucidate this role are now in progress.

Acknowledgment. We wish to thank Drs. C. J. Carrano and W. R. Harris and Mr. V. L. Pecoraro for many helpful discussions. T.P.T. gives special thanks to Ms. M. J. Kappel for assistance with the nonlinear least-squares refinement. This research is supported by the National Institutes of Health through Grant No. AI 11744.

(46) Cooper, S. R.; McArdle, J. V.; Raymond, K. N. *Proc. Natl. Acad. Sci. U.S.A.* **1978**, *75*, 3551.
(47) Straka, J. G.; Emery, T. *Biochim. Biophys. Acta* **1979**, *569*, 277.
(48) Brown, K. A.; Ratledge, C. *FEBS Lett.* **1975**, *53*, 262.
(49) Ernst, J. F.; Winkelmann, G. *Biochim. Biophys. Acta* **1977**, *500*, 27.
(50) Sirivech, S.; Driskell, J.; Frieden, E. *J. Nutr.* **1977**, *107*, 739.

Ion-Beam Studies of the Reactions of Atomic Cobalt Ions with Alkenes

P. B. Armentrout, L. F. Halle, and J. L. Beauchamp*[1]

Contribution No. 6311 from the Arthur Amos Noyes Laboratory of Chemical Physics, California Institute of Technology, Pasadena, California 91125. *Received January 21, 1981*

Abstract: An ion-beam apparatus is employed to study the reactions of singly charged cobalt positive ions with 12 alkenes. While ethene and propene undergo no exothermic reactons, two processes are observed for larger olefins. One reaction yields cobalt ion alkadiene complexes and either methane or H_2. The second process involves cleavage of the alkene into two smaller olefins, one of which remains bound to Co^{+}. A mechanism involving oxidative addition of an allylic C–C or C–H bond to the metal as the initial step is proposed to account for all observed products. Subsequent formation of a cobaltacyclobutane species is postulated for several of the cleavage reactions.

In a recent article (hereafter referred to as I),[2] the reactions of Co^{+} with saturated hydrocarbons were reported. Exothermic reactions were observed to yield cobalt ion–alkene complexes, and in some systems, small amounts of cobalt ion–alkadiene complexes. At higher collision energies, these latter products often predominated. It was postulated that the alkadiene complexes resulted from subsequent reactions of the initially formed alkene complexes. A simplified potential energy surface for one such system is shown in Figure 1. It demonstrates how the alkene complex intermediate can also be accessed by direct reaction of the alkene with cobalt ions. An examination of such reactions would provide a test of the hypothesis made in I as well as extend the study of the general reactivity of Co^{+} with hydrocarbons.

Using an ion-beam apparatus, the reactions of Co^{+} with 12 alkenes have been studied in the present work. It is found that these reactions do indeed yield cobalt ion alkadiene complexes. In addition, cleavage of the alkene into smaller alkenes, one of which remains bound to Co^{+}, is also observed. These unexpected cleavage reactions provide an explanation for several products reported in I which appeared anomalous. A mechanism involving initial formation of an allyl complex is shown to account for all products observed. For some reactions, subsequent conversion

0002-7863/81/1503-6624$01.25/0